Attaining and maintaining criticality in a neuronal network model

Article *in* Physica A: Statistical Mechanics and its Applications · April 2013

DOI: 10.1016/j.physa.2012.11.013

2 authors:

Jiayi Peng
University of Hawai'i System
13 PUBLICATIONS **107** CITATIONS
SEE PROFILE

John M. Beggs
Indiana University Bloomington
76 PUBLICATIONS **2,161** CITATIONS
SEE PROFILE

Physica A 392 (2013) 1611–1620

Contents lists available at SciVerse ScienceDirect

Physica A

journal homepage: www.elsevier.com/locate/physa

Attaining and maintaining criticality in a neuronal network model

Jiayi Peng [a,*], John M. Beggs [b]

[a] 121 King Street #4, Chappaqua, NY 10514, USA

[b] Department of Physics, Indiana University, Bloomington, IN 47405, USA

ARTICLE INFO

Article history:
Received 31 May 2012
Received in revised form 19 September 2012
Available online 30 November 2012

Keywords:
Neuronal network
Self-organized criticality
Neuronal avalanche
Data collapse
Cellular automaton

ABSTRACT

We propose a cellular automaton model for neuronal networks that combines short-term synaptic plasticity with long-term metaplasticity. We investigate how these two mechanisms contribute to attaining and maintaining operation at the critical point. We find that short-term plasticity, represented in the model by synaptic depression and synaptic recovery, is sufficient to allow the system to attain the critical state, if the level of plasticity is properly chosen. However, it is not sufficient to maintain the criticality if the system is perturbed. But the long time scale change in the short-term plasticity, a change in the way synaptic efficacy is modified, allows the system to recover from perturbation. Working together, these two time scales of plasticity could help the system to attain and maintain criticality, leading to a self-organized critical state.

1. Introduction

A major task at the interface of neuroscience and physics is to determine the general principles by which groups of neurons collectively process information. Recently, experimental evidence has accumulated that networks of cortical neurons can operate at a critical point, poised between a subcritical phase where activity is damped and a supercritical phase where activity is amplified [1–3]. At the critical point between these phases, activity forms avalanches of all sizes and is distributed as a power law [1]. Several studies, both computational [1,4–8] and experimental [9,10], have also shown that a broad range of information processing functions would be optimized at the critical point [11–13]. The idea that networks of cortical neurons self-organize toward the critical point to optimize information processing has been called "the criticality hypothesis" [11]. As this hypothesis has gained experimental support, several models have been proposed to explain how synaptic plasticity could cause neuronal networks to self-organize toward the critical point [14–21].

The idea of self-organization is widely accepted in neuroscience, and has been shown, for example, to be responsible for the development of appropriate synaptic connections in sensory [22] and motor systems [23] over the course of weeks. Changes in synaptic strength are also thought to underlie recovery from neurological damage such as that caused by a stroke [24,25]. Some studies have even shown that developing neural networks begin to produce power-law distributions of avalanche sizes only after several weeks of synaptic formation and pruning [26,27].

In contrast, the idea of self-organized criticality (SOC) has had a mixed reception in physics [28–30]. The prototypical model of SOC is the "sand pile model" [31]. Here, simulated grains of sand are slowly dropped onto a surface and begin to form a pile. When this pile becomes too steep, avalanches of sand are triggered, making the pile less steep. When the pile has a shallow slope, it accumulates more sand to become steeper. This interplay of avalanches and accumulation, so it is argued by proponents of SOC, can lead the system to self-organize toward a critical point where avalanches of all sizes will occur [32]. Here, the shape of the sand pile contains some memory of previous activity and is thought to play a crucial role

* Corresponding author.
E-mail address: jiayi314@gmail.com (J. Peng).

0378-4371/$ – see front matter © 2012 Elsevier B.V. All rights reserved.
doi:10.1016/j.physa.2012.11.013

in guiding the system toward the critical point. Indeed, simulation work demonstrated that this and similar models would produce power-law distributions of avalanche sizes [33]. Proponents of SOC agree that under some parameter choices the system will not be critical, but maintain that for a limited range of parameter values the system will display self-organization toward criticality. Critics of this work have argued that, while these models for some parameter choices appear to be critical, they are probably not self-organizing [33]. In this view, the memory of activity does not play a role in driving the system toward the critical point. Instead, the choice of initial parameters determines whether or not the system will operate at the critical point.

Given this background, this raises the question of how the brain, a biologic system, would get to the critical point. Biological systems are notoriously noisy and subject to constant perturbations. Synapses often change strength, through both short-term and long-term synaptic plasticity. This changing system would seem unlikely to reach the narrow region of the critical point on its own.

Despite the challenges, there has been some progress in our understanding of how SOC is reached in neuronal systems. In 2007, Levina et al. [17] proposed a model with short-term plasticity using negative feedback mechanisms which could help regulate the system to attain a critical point. A large avalanche reduces the neuronal activities in the system through synaptic depression, decreasing the odds of another large avalanche and increasing the chance of smaller avalanches. On the other hand, a small avalanche would leave many synapses in the system unused. Over time, these unused synapses recover their strengths through another mechanism — synaptic recovery — setting the stage for another large avalanche. This is one version of SOC, arrived at through the interplay of synaptic depression and synaptic recovery.

What then would be the role of long-term plasticity? Tetzlaff et al. [27] showed that, during development, dissociated cultures gradually approach the critical point. First they are subcritical, then supercritical, then finally critical. This suggests that long-term changes in synaptic strength are occurring, but not interfering with the path to criticality. They model this through activity-dependent axonal growth that would cause homeostatic regulation. Another theoretic work, proposed by de Arcangelis et al. [16], reached a similar conclusion that SOC is possible only after synaptic pruning.

Thus, both long-term and short-term plasticity could drive the network to the critical point. But we know that both are present in real neuronal networks. How could synaptic plasticity at both of these time scales work together? Would it be possible to combine both in one model and partition their effects? To investigate this, we build upon the model of Levina et al. [17], where time scale separation is assumed. On the short time scale, synaptic depression and synaptic recovery are used as short-term plasticity. Here, on the long term scale, we introduce a *plasticity* of the short-term plasticity ("metaplasticity") [34], and allow the synaptic parameter to be modified over the long time scale. This idea was inspired by the self-organizing branching model of Zapperi et al. [35]. We investigate how these two mechanisms contribute to attaining and maintaining operation at the critical point. We find that short-term plasticity, if properly chosen, is sufficient to allow the system to attain the critical state. However, it is not sufficient to maintain the criticality if the system is perturbed. The long time scale change in short-term plasticity allows the system to recover from perturbation. Working together, these two time scales of plasticity could help the system to attain and maintain criticality.

The paper is organized as follows. In Section 2, we introduce the model and the methods of how we record data from the simulations. In Section 3, we present the results and our analysis. In Section 4, we conclude the paper with discussions.

2. Methods

2.1. Model

Consider a two-dimensional square lattice of N neurons with open boundary conditions in both the x and y directions. Each neuron is represented by a membrane potential h_i in the range $[0, 1]$. A neuron interacts with its four nearest neighbors through a synaptic strength w_{ij} between neurons i and j ($w_{ij} \neq w_{ji}$, meaning that the synaptic strength is asymmetric). Once its membrane potential is above the threshold of 1, a neuron fires and sends a spike to its neighbors, causing a change in their membrane potentials. Our model is a continuous cellular automaton model. The system is driven by external inputs at a sufficiently slow pace, meaning that driving only happens when there is no neuronal avalanche. In other words, there is a separation of time scales. The following update rules list how the simulation is carried out on the short time scale (steps 1–6) and on the long time scale (step 7).

- *Step* (1) *Driving*. The system is driven by random external inputs ξ_i whose range is between 0 and 0.1. Slow-driving is implemented if and only if all membrane potentials are below the threshold of 1. Driving occurs at only one neuron chosen randomly among the N neurons.

$$h_i = h_i + \xi_i. \tag{1}$$

- *Step* (2) *Firing*. If a neuron's membrane potential h_i is above the threshold of 1, then the neuron spikes, and it is reset to

$$h_i = h_i - 1. \tag{2}$$

- *Step* (3) *Integration*. The four nearest neighbors of the firing neuron, represented by h_j, integrate the membrane potential released by the firing neuron proportional to the synaptic strength between them, w_{ij}:

$$h_j = h_j + 1/NN^* w_{ij}, \tag{3}$$

where NN is the number of neighbors of the firing neuron.

- *Step* (4) *Synaptic depression*. Immediately after the synaptic strength is used, it is decreased by a certain percentage u (following Levina et al. [17]):

$$w_{ij} = w_{ij} - u^* w_{ij}. \tag{4}$$

- *Step* (5) *Synaptic recovery*. All synaptic strengths in the system recover by a constant percentage c (recovery rate) of the difference between the current synaptic strength w_{ij} and a target synaptic strength T:

$$w_{ij} = w_{ij} + c^*(T - w_{ij}). \tag{5}$$

The implication of this rule is that the greater the difference between T and w_{ij}, the faster the synaptic weight recovers.

- *Step* (6) *Avalanche process*. Repeat steps 2–5 until no neuron's membrane potential is above 1 (when an avalanche is over). An avalanche is defined as a period of activity that is initiated by an external input and is terminated when no further neuron becomes activated. When the avalanche is over, it is said that one time step on the long time scale is completed.
- *Step* (7) *Metaplasticity*. On the long time scale, borrowing an idea from the self-organized branching process (SOBP) model introduced by Zapperi et al. [35], we monitor the number of neurons in the layer on the boundary that have fired in the previous avalanche process. Assuming that that number is X, the parameter u in Eq. (4) is adjusted according to the following equation:

$$u(t+1) = u(t) - (1 - X)/N, \tag{6}$$

where t is the time step on the long time scale, and N is the number of neurons in the network. The updated u will be kept constant throughout all the time steps on the short time scale (steps 1–6) until the next time step on the long time scale.

The simulations repeat steps 1–7 until a desired number of iterations is achieved. Since this study is trying to analyze the role of short-term plasticity and the role of long-term metaplasticity, not all simulations are done with step 7. In fact, for a large portion of our results, we are going to show that short-term plasticity, if properly chosen, is sufficient to allow the system to attain the critical point. Thus step 7 will be skipped in these simulations. We will show that step 7 is necessary for the system to maintain the criticality.

All simulations start with random membrane potentials (h_i) uniformly distributed in [0, 1] and random synaptic strengths (w_{ij}) uniformly distributed in [0, 0.25]. We run the simulation according to the above rules for a long time period before we record avalanches to make measurements. Depending on the system size we use, the time period before measurement (pre-measurement time) ranges from two million time steps to 48 million time steps (on the long time scale). The measurement time usually lasts for one to four million time steps. We run the simulation for a long time to overcome the effects of initial conditions. In particular, many time steps are required to overcome critical slowing down of the system which occurs near the critical point. To decide if a pre-measurement time is long enough to overcome the initial condition and lead the system to a steady state, we simply double the pre-measurement time steps to see if we can obtain the same avalanche size distribution as we obtained before doubling the time steps. We find that running a few hundreds of thousands of time steps is sufficient for this purpose for all system sizes studied here.

Our model parameters can be related to the model parameters in the Levina–Herrmann–Geisel (LHG) model [17]. The parameter c from Eq. (5) equals $1/(\tau\nu N)$ of the LHG model with $\tau = 1$ and $1 < \nu \ll N$; our model parameter T from Eq. (5) equals α/u of the LHG model:

$$c = 1/(\tau\nu N) \tag{7}$$

$$T = \alpha/u. \tag{8}$$

From now on, we will use the symbols of the LHG model (ν, u, α) when referring to our model parameters. Throughout the paper, we will mostly change the model parameter u (control parameter) while keeping the others constant.

2.2. Avalanches and avalanche size distribution

An avalanche process starts when a neuron is driven to fire (step 2 in the model) and ends when no neuron has a membrane potential above the threshold. The avalanche size is the number of firings during the avalanche process, and the avalanche duration is the number of time steps (on the short time scale) passed in the process. To record avalanche sizes, we count the number of neurons which fired in the avalanche process (a neuron can be counted more than once if it fires more than once during the avalanche process). At the same time, to record the avalanche duration, the number of time steps (on the short time scale) is recorded. The avalanche size distribution, described by the probability density function $P(s)$, is obtained by calculating the ratio of the number of occurrences of avalanches with size s to the total number of avalanches recorded during the measurement time.

2.3. Power-law exponents

We use both the least squared (LS) error and the Kolmogorov–Smirnov (KS) estimate to determine the exponent of a power-law distribution [36]. The critical value of u is obtained by minimizing the KS error using the software package provided in Ref. [36].

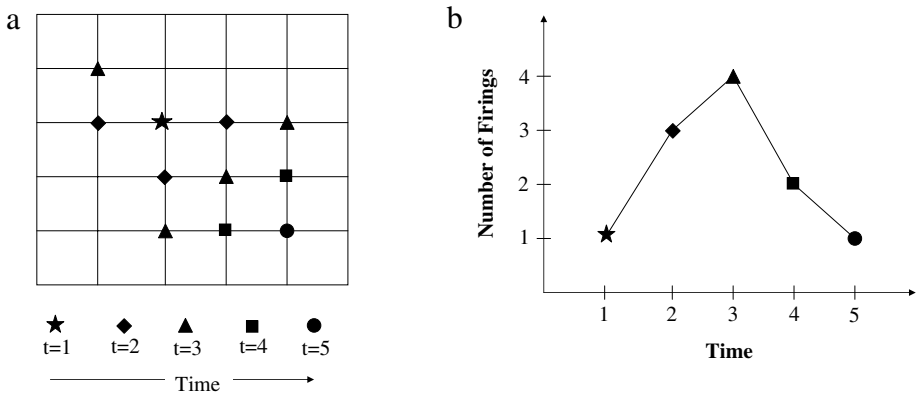

Fig. 1. (a) An avalanche, starting with the "star" at time step $t = 1$, propagates to the "diamond" at time step $t = 2$, and then to the "triangle", the "square", and the "circle" at $t = 3$, $t = 4$, and $t = 5$ (on the short time scale). The avalanche size is 11, since there are 11 neuronal firings, and the avalanche duration is 5 in this example. (b) Avalanche shape, defined as the curve of the number of firings plotted against the time step on the short time scale.

2.4. Avalanche shapes

Fig. 1 illustrates how an avalanche shape is defined. In Fig. 1(a), an avalanche, starting at the "star" at time step (on the short time scale) $t = 1$, propagates to the "diamond" at $t = 2$, and then to the "triangle", the "square", and the "circle" at $t = 3$, $t = 4$, and $t = 5$, respectively. In this example, the avalanche size is 11 and the avalanche duration is 5. The avalanche shape is defined as the temporal shape of the number of firings (y-axis) plotted against the time step (x-axis), as shown in Fig. 1(b). To minimize the noise and to get a smooth shape curve for a given duration, we averaged the shapes of all the avalanches with the same duration collected during the measurement time period.

2.5. Perturbing the critical state

We first let the model run for 4,000,000 time steps (on the long time scale) under parameters known to lead to criticality (for system size $N = 4096$), allowing the pattern of synaptic connection strengths to become well established. Next, we perturb the critical state by switching parameter u to a value that is known to produce a non-critical distribution. We then run the model for another 4,000,000 time steps in order to allow the system to settle into a new state. We want to see if the new state is critical or not. To check the new state, we record the avalanches for an additional 2,000,000 time steps to see if the avalanche size distribution is different from that of the critical state. If a system is truly a self-organized critical system, it would return to criticality after perturbation and the avalanche size distribution would show a power-law distribution identical to that of the critical state. Otherwise, it would indicate that the criticality is unsustainable to perturbation.

3. Results

We will first show that the short-term plasticity alone is sufficient to attain a critical state, as long as the model parameters are properly chosen. But the criticality is not maintained if the system is perturbed. Therefore, the results in Section 3.1 through 3.6 are obtained by skipping step 7 described in Section 2.

3.1. Avalanche size distribution

Fig. 2 shows the size distributions for three sets of model parameters on a system size of $N = 4096$, corresponding to three different states the system can attain: critical, subcritical, and supercritical. All three curves show power-law decays for small values of avalanche size. For $u = 0.34$, there is a fast drop off from the power-law line at larger avalanche sizes, showing that the system is at a subcritical state. For $u = 0.14$, there is a "bump" for larger avalanche size values, indicating that the system is at a supercritical state. In the intermediate state, $u = 0.24$, the size distribution has the longest range of avalanche size for the power-law form, corresponding to a critical state. The power-law exponent of the critical size distribution, $P(s) \sim s^{-\tau}$, was estimated to be -1.55 ± 0.02, which is slightly larger than the exponent of -1.5 found in the experiment using rat cortical slices *in vitro* [1].

3.2. Finite-size scaling

A power-law size distribution does not always indicate that a system is critical. A critical system is also scalable with different system sizes. To test this, in Fig. 3(a) we show the size distributions for four different system sizes when the system is at the critical state. In Fig. 3(b) we show the finite-size scaling by data collapsing them onto one curve.

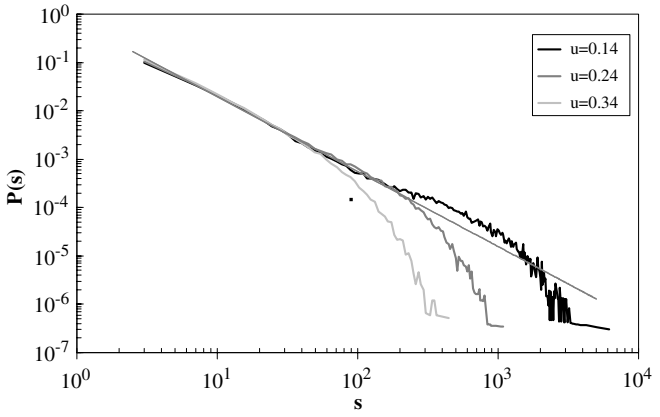

Fig. 2. Avalanche size distributions for $N = 4096$, $\nu = 75$, $\alpha = 5.6$, and different values of u, showing that the system is in a supercritical ($u = 0.14$), critical ($u = 0.24$), and subcritical ($u = 0.34$) state, illustrated as the black, the dark gray and the light gray curves from right to left, respectively. The straight line has a slope of -1.55, which is the size distribution exponent.

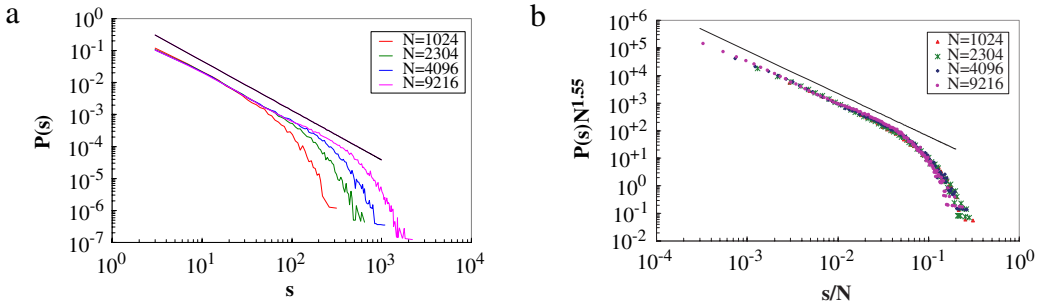

Fig. 3. (a) Avalanche size distributions for different system sizes when the system is at a critical state. (b) Finite-size scaling of the distributions in (a). The line has a slope of -1.55 in both (a) and (b).

3.3. Scaling of non-critical size distributions

In critical phenomena, even non-critical size distributions could be scaled together. For example, in the theory of percolation [37], a non-critical size distribution could be scaled using a reduced parameter s/s_0, where s_0 is the typical cluster size (related to the correlation length), for both subcritical and supercritical states. However, in percolation, in order to scale the size distribution in the supercritical state, one needs to exclude the infinite component. Here we have a situation similar to percolation, but removing the infinite component is difficult in this case. We have attempted to remove avalanches that spanned from one border to the opposite, as done in percolation models, but this method resulted in a distribution where the data still peaks at the end, different from a distribution resembling a subcritical distribution one would get in percolation after the infinite component is removed. This difference may be caused by the fact that the supercritical state in the percolation model has a different distribution than the distribution of the supercritical state in the current model; the former has a dip and a sharp peak at the end while the latter has a broader tail with no dip, which makes deciding where to remove "the infinite component" difficult. Nevertheless, we were able to scale the size distributions in the subcritical state. In Fig. 4(a), we show three subcritical size distributions along with the critical one. In Fig. 4(b), the three subcritical distributions are data collapsed onto one curve using the reduced parameter s/s_0, with $s_0 = (u - u_c)^{-0.5}$ in the horizontal axis, and $P(s)s_0^{\tau} = P(s)^*(u - u_c)^{-0.775}$ in the vertical axis.

3.4. Avalanche shape scaling

To further verify the critical state, we analyze the scaling properties of avalanche shapes. It is argued that the temporal avalanche shapes are scalable if the system is at a critical state [3,38]. From the theory of critical phenomena, scaling works well near the critical point. In Fig. 5, we show that the shapes can be collapsed onto one curve using an exponent $\zeta = 0.85$ for shapes with durations from 5 to 20 when the system is at the critical state. However, we were unable to extend the shape scaling study to the non-critical states, since the range of duration that can be scalable is very limited there.

The shape collapse in the simulation shows that an avalanche shape can be expressed generally as

$$s(t, D) = D^{\zeta} F(t/D), \tag{9}$$

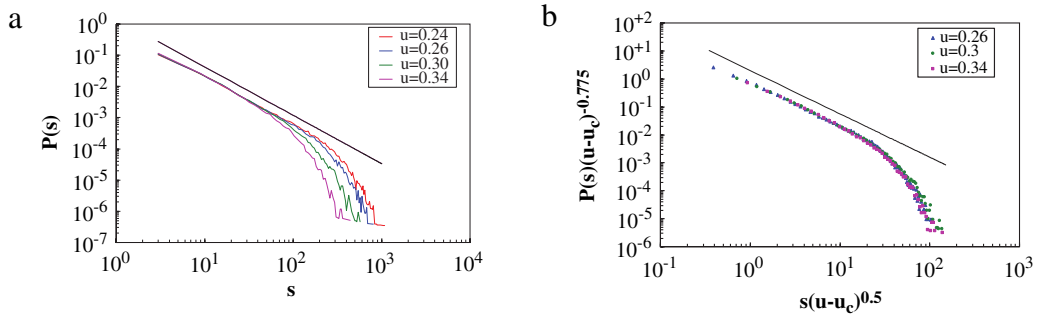

Fig. 4. (a) Avalanche size distributions for $N = 4096$ and different values of u in the subcritical state. (b) Avalanche size distributions in (a) are scaled to one curve using reduced size parameter s/s_0, with $s_0 = (u - u_c)^{-0.5}$. The line has a slope of -1.55 in both (a) and (b).

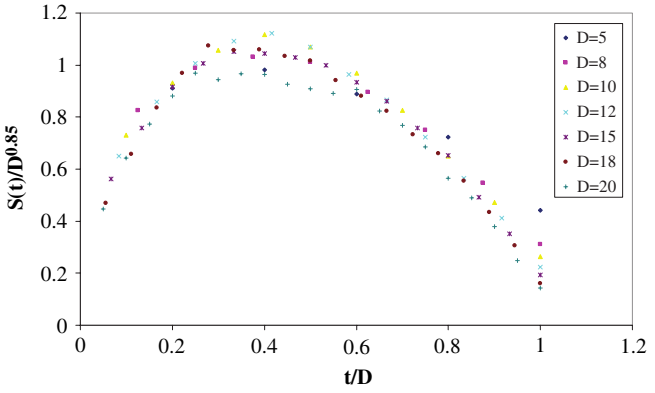

Fig. 5. Scaling of avalanche shapes when the system is at a critical state ($N = 4096$, $\nu = 75$, $u = 0.24$ and $\alpha = 5.6$).

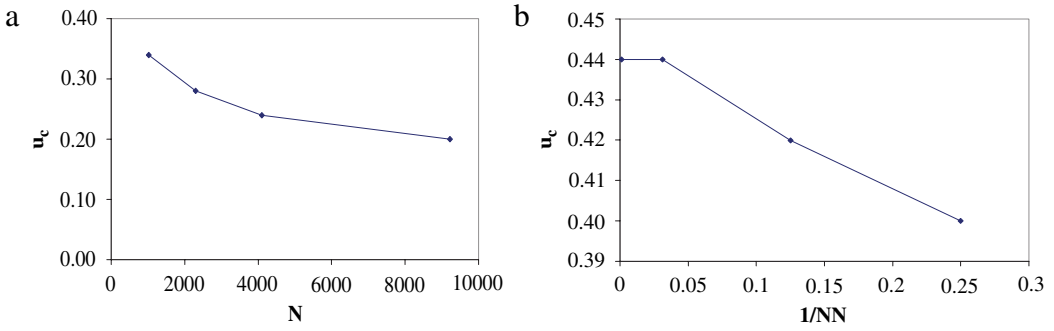

Fig. 6. (a) Relationship between u_c and N. (b) Relationship between u_c and the (inverse of) number of neighbors (NN). The model parameters are $N = 1024$, $\nu = 75$, and $\alpha = 5.6$ on randomly connected networks with fixed number of outgoing neighbors ($NN = 4$, 8, 32, and 1023).

where t is the time (on the short time scale) elapsed since the avalanche start (see Fig. 1(b)), D is the duration of the avalanche, and F is a function that determines the avalanche shape profile. Since the function F has infinitely more degrees of freedom than one given number, a scaling function has more information than a power-law exponent.

3.5. Impact of system size and network structure

We have tested that changing both the system size and the network structure has no effect on the existence of three states. The only impact of the system size and the network structure is that they shift the critical value u_c. In Fig. 6(a), we show that u_c is becoming smaller as the system size increases. In Fig. 6(b), we show that, as the number of neighbors (NN) decreases, the critical value of u is decreasing. Here, we have extended our model to random networks in order to study the effect of NN. We used random networks where each neuron has the same fixed number of outgoing links to other randomly picked neurons. When $NN = N - 1$, the random network becomes a fully connected network.

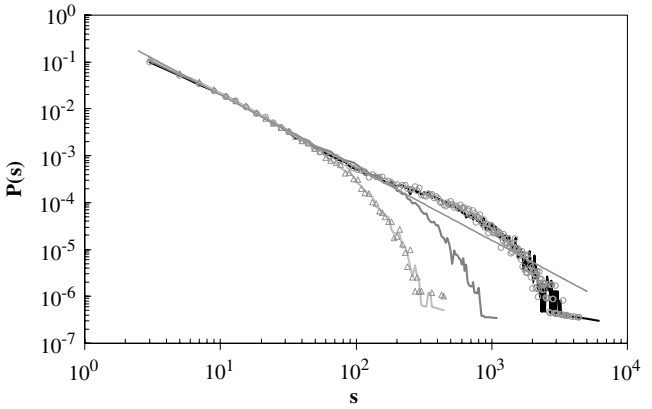

Fig. 7. The system is first driven to a critical state by using $N = 4096$, $\nu = 75$, $\alpha = 5.6$, and $u = 0.24$ for four million time steps (on the long time scale). Then the model parameter u is switched to subcritical value $u = 0.34$ or supercritical value $u = 0.14$, and the system runs for another four million time steps before the avalanche size distribution is recorded for an additional two million time steps. The size distribution thus recorded is shown in "triangles" and "circles" for subcritical and supercritical perturbations, respectively. The black, dark gray, and light gray curves are the original size distributions without perturbation (*Source:* Taken from Fig. 2).

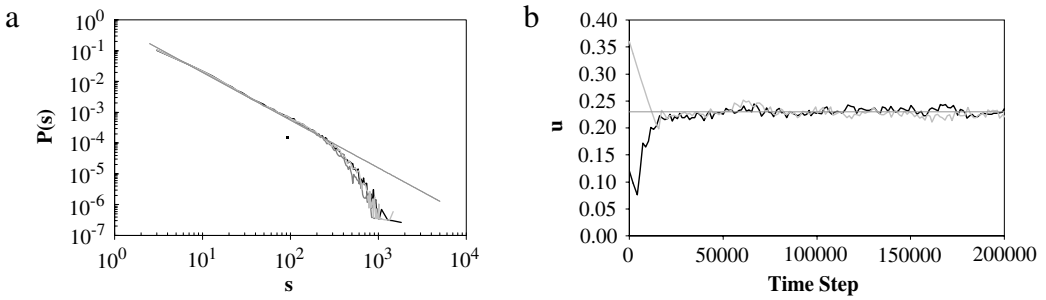

Fig. 8. (a) Avalanche size distributions for systems starting with different initial values of u, $u(0) = 0.12$ (black) and $u(0) = 0.36$ (light gray). The systems are undergoing the long-term metaplasticity process of Eq. (6). For comparison, the dark gray curve is the size distribution at the critical state when u was kept constant at $u = 0.24$. (*Source:* Taken from Fig. 2). The other model parameters are $N = 4096$, $\nu = 75$, and $\alpha = 5.6$ for all curves. (b) $u(t)$ versus time step for the two systems in (a) starting with different initial values of u, $u(0) = 0.12$ (black) and $u(0) = 0.36$ (light gray). The value of $u(t)$ converges to $u = 0.23$, represented by the horizontal line.

3.6. Perturbing the critical state

To see if the criticality created by the short-term plasticity is still maintained if it is perturbed, we first run the system to a critical state with parameters known to lead to the critical state ($N = 4096$, $\nu = 75$, $u = 0.24$, and $\alpha = 5.6$). Then, the parameter u is switched to a value that is known to produce a non-critical results ($u = 0.34$ or $u = 0.14$). In Fig. 7, we compare the size distributions obtained in this manner (see Section 2.5 — *Perturbing the critical state*) to the size distributions obtained from running the system with constant non-critical values of u for all time steps ($u = 0.34$ and $u = 0.14$). It is clear from Fig. 7 that the results from perturbing the critical state are almost identical to the non-perturbed results. There is no indication that the system could pull itself back into criticality after perturbation.

3.7. Long-term metaplasticity

Now, if we let the system undergo the long-term metaplasticity process of Eq. (6), we can obtain the power-law distribution no matter what the initial value of u is. Fig. 8(a) shows the avalanche size distributions for systems starting with different initial values of u, $u(0) = 0.12$ and $u(0) = 0.36$. The dark gray curve is the size distribution at the critical state taken from Fig. 2 when u was kept constant at $u = 0.24$. It is clear that the power-law distribution is maintained by the long-term metaplasticity process. Fig. 8(b) shows that the value of u converges to a value of 0.23 (which is very close to our earlier estimate of u_c for this system) after a few tens of thousands of time steps on the long time scale, regardless of where the parameter u started.

It is no surprise that this mechanism works, since it is one of the criteria offered by Sornette [39] for a system to evolve into a self-organized critical state. But we want to point out that, in biological systems, long-term cooperation does happen, and this mechanism may very well represent the metaplasticity on the long time scale, albeit in a simple way.

4. Discussion and conclusion

4.1. Summary of main findings

In this paper, we have studied the roles of short-term plasticity and long-term metaplasticity in attaining and maintaining the critical state. We find that short-term plasticity could lead to a critical state if the model parameters are set at the critical values. However, perturbation, which is common in biological systems, can easily shift the system to a non-critical state. The long-term metaplasticity, introduced here as a plasticity of the short-term plasticity, allows the synaptic parameter to be modified over the long time scale and allows the system to recover from perturbation. Working together, these two time scales of plasticity could help the system to attain and maintain criticality, leading to a self-organized critical state.

4.2. Validity and limitations

Our results should in no way be taken as evidence that self-organized criticality does not exist with short-term plasticity alone. We merely examined our own cellular automaton model. Although this model was inspired by the LHG model [17], it is not exactly the numerical discretization of their model which is in partial differential equation form. It is possible that our numerical evidence on the perturbation, no matter how long we have run, may not be long enough for the system to return to the critical state. This is especially true if the route to criticality is a slow process. The issue of which form of criticality, self-organized or not, is obeyed by the brain is very intriguing, as recently pointed out in Ref. [40], and we believe the topic deserves more work.

4.3. Comparison to other work

Our model is an integrate-and-fire model with plasticity. Models with integrate-and-fire oscillators (IFOs) are probably the simplest models for neuronal network modeling. In Ref. [41], Hopfield and Herz studied several different types of IFO in a locally coupled network and found that, when the resistance of the oscillator goes to infinity (as assumed in our model), the model (Model C in Ref. [41]) falls into the sand pile SOC model. In other types of models, Hopfield and Herz [41] found that the system ends with synchronized firings across all neurons. In a slightly different setting, Corral et al. [42] found that, depending on the parameters used, the system can be in a critical state, or a macroscopically synchronized state. The above-mentioned models differ from ours in the sense that there was no plasticity present in these models, either short-term or long-term, as all the synaptic strengths are constant.

The continuous cellular automaton nature of our model is similar to that of an earthquake model proposed by Olami, Feder, and Christensen (OFC) [43]. In 1996, Lise and Jensen [44] claimed that the random-neighbor OFC model is an SOC model for a range of model parameters. Later, Broker and Grassberger [45], and Chabanol and Hakin [46] showed that the random-neighbor OFC model is critical only when the model parameter is at a critical value such that the system is conserved. The update rules in the OFC model are different from ours because the energy redistribution after a spike is handled by a constant dissipation parameter, while in our model the redistribution of membrane potential is changing due to the short-term plasticity and the long-term metaplasticity.

4.4. Biological plausibility

The short-term plasticity that is captured by the parameter u seems plausible, as short-term plasticity has been observed in experiments on cortical synapses. So the short-term changes that lead to the critical state, as proposed by LHG [17], seem reasonable. On the longer time scale, recovery from perturbation depends on metaplasticity. Metaplasticity has been observed in studies of long-term synaptic potentiation and depression [47,48]. To implement metaplasticity of the synaptic recovery variable u on the long time scale, the model used a count of the number of active neurons on the boundary of the system. While this might seem biologically implausible in detail, the general idea of negative feedback operating over long time scales has abundant biological support. For example, Turrigiano and colleagues [49] have shown that networks of neurons homeostatically regulate the firing rate and synaptic strength in response to external perturbations so as to bring network firing rates into a target zone. Mechanisms like this could also conceivably operate on short-term plasticity or other variables so as to bring the network to the critical state after perturbation [20,21].

4.5. Implications for future models

As recent experiments seem to suggest that neural tissue can operate at the critical point [1–3], it is natural to ask whether the brain is an example of SOC or not [50]. There is evidence that cultured neuronal networks do not initially produce power-law distributions of avalanche sizes, but that over weeks they develop to a state where such power-law distributions are common [26,27]. Over this period of weeks, typically large numbers of synaptic connections are established, change strength and are pruned [51,52]. During neural development, many relevant parameters in the system are undergoing large changes in value, yet the network eventually arrives at the critical state. Taken together, this information strongly suggests that

neural tissue would belong to the class of SOC systems that display stability with respect to perturbations. If this conclusion is correct, it would further suggest that models that do not demonstrate stability with respect to perturbations are incomplete models of criticality in neural tissue.

Future work therefore should concentrate on models that can account for the large and persistent changes in synaptic strength that are known to occur. The approach taken by de Arcangelis and colleagues [16] was along this line, since in their model synaptic pruning was included and the network topologic structure was altered as a result. Hopefully, such models will in turn suggest experiments that will constrain the types of mechanisms that could be responsible for driving the brain to the critical point and maintaining it there. An understanding of these mechanisms would be especially useful, as evidence is beginning to accumulate that several neuropathologies are associated with a failure to operate at the critical point [53–56].

Acknowledgments

J.P. would like to thank Richard Goodman, Carol DiGuglielmo, and Trudy Gessler for their help and support. J.M.B. was supported in part by an NSF PoLS grant (1058291).

References

[1] J.M. Beggs, D. Plenz, Neuronal avalanches in neocortical circuits, J. Neurosci. 23 (2003) 11167.
[2] T. Peterman, T.C. Thiagarajan, M.A. Lebedev, M.A.L. Nicolelis, D.R. Chialvo, D. Plenz, Spontaneous cortical activity in awake monkeys composed of neuronal avalanches, Proc. Natl. Acad. Sci. 106 (2009) 15921.
[3] N. Friedman, S. Ito, B. Brinkman, M. Shimono, R.E. DeVille, K. Dahmen, J.M. Beggs, T.C. Butler, Universal critical dynamics in high resolution neuronal avalanche data, Phys. Rev. Lett. 108 (2012) 208102.
[4] N. Bertschinger, T. Natschläger, Real-time computation at the edge of chaos in recurrent neural networks, Neural Comput. 16 (2004) 1413.
[5] W. Maass, T. Natschläger, H. Markram, Real-time computing without stable states: a new framework for neural computation based on perturbations, Neural Comput. 14 (2002) 2531.
[6] C. Haldeman, J.M. Beggs, Critical branching captures activity in living neural networks and maximizes the number of metastable states, Phys. Rev. Lett. 94 (2005) 058101.
[7] O. Kinouchi, M. Copelli, Optimal dynamical range of excitable networks at criticality, Nat. Phys. 2 (2006) 348.
[8] T. Tanaka, T. Kaneko, T. Aoyagi, Recurrent infomax generates cell assemblies, neuronal avalanches and simple cell-like selectivity, Neural Comput. 21 (2009) 1038.
[9] W.L. Shew, H. Yang, T. Petermann, R. Roy, D. Plenz, Neuronal avalanches imply maximum dynamic range in cortical networks at criticality, J. Neurosci. 29 (2009) 15595.
[10] W.L. Shew, H. Yang, S. Yu, R. Roy, D. Plenz, Information capacity and transmission are maximized in balanced cortical networks with neuronal avalanches, J. Neurosci. 31 (2011) 55.
[11] J.M. Beggs, The criticality hypothesis: how local cortical networks might optimize information processing, Phil. Trans. R. Soc. A 366 (2008) 329.
[12] D. Plenz, T.C. Thiagarajan, The organizing principles of neuronal avalanches: cell assemblies in the cortex? Trends in Neurosci. 30 (2007) 101.
[13] D.R. Chialvo, Emergent complex neural dynamics, Nat. Phys. 6 (2010) 744.
[14] D.R. Chialvo, P. Bak, Learning from mistakes, Neurosci. 90 (1999) 1137.
[15] P. Bak, D.R. Chialvo, Adaptive learning by external dynamics and negative feedback, Phys. Rev. E 63 (2001) 031912.
[16] L. de Arcangelis, C. Perrone-Capano, H.J. Herrmann, Self-organized criticality model for brain plasticity, Phys. Rev. Lett. 96 (2006) 028107.
[17] A. Levina, J.M. Herrmann, T. Geisel, Dynamical synapses causing self-organized criticality in neural networks, Nat. Phys. 3 (2007) 857.
[18] A. Levina, J.M. Herrmann, T. Geisel, Phase transitions towards criticality in a neural system with adaptive interactions, Phys. Rev. Lett. 102 (2009) 118110.
[19] L.F. Abbott, R. Rohrkemper, A simple growth model constructs critical avalanche networks, Prog. Brain Res. 165 (2007) 13.
[20] D. Hsu, J.M. Beggs, Neuronal avalanches and criticality: a dynamical model for homeostasis, Neurocomputing 69 (2006) 1134.
[21] D. Hsu, A. Tang, M. Hsu, J.M. Beggs, Simple spontaneously active Hebbian learning model: homeostasis of activity and connectivity, and consequences for learning and epileptogenesis, Phys. Rev. E 76 (2007) 041909.
[22] D.H. Hubel, T.N. Wiesel, Receptive fields of single neurones in the cat's striate cortex, J. Physiology 148 (1959) 574.
[23] T. Nakamura, K. Kiyono, K. Yoshiuchi, R. Nakahara, Z.R. Struzik, et al., Universal scaling law in human behavioral organization, Phys. Rev. Lett. 99 (2007) 138103.
[24] T.P. Pons, P.E. Garraghty, M. Mishkin, Lesion-induced plasticity in the somatosensory cortex of adult macaques, Proc. Natl. Acad. Sci. 85 (1988) 5279.
[25] B.B. Johansson, Brain plasticity and stroke rehabilitation, Stoke 31 (2000) 223.
[26] C.V. Stewart, D. Plenz, Homeostasis of neuronal avalanches during postnatal cortex development in vitro, J. Neurosci. Meth. 169 (2008) 405.
[27] C. Tetzlaff, S. Okujeni, U. Egert, F. Wörgötter, M. Butz, Self-organized criticality in developing neuronal networks, PLoS Comput. Biol. 6 (2010) e1001013.
[28] G. Grinstein, in: A. McKane, et al. (Eds.), Scale Invariance, Interfaces and Non-Equilibrium Dynamics, in: NATO Advanced Study Institute, Series B: Physics, vol. 344, Plenum, New York, 1995.
[29] D. Sornette, A. Johansen, I. Dornic, Mapping self-organized criticality onto criticality, J. Physique I 5 (1995) 325 (France).
[30] A. Vespignani, S. Zapperi, V. Loreto, Renormalization on non-equilibrium systems with critical stationary state, Phys. Rev. Lett. 77 (1996) 4560.
[31] P. Bak, C. Tang, K. Wiesenfeld, Self-organized criticality: an explanation of the 1/f noise, Phys. Rev. Lett. 59 (1987) 381.
[32] P. Bak, How Nature Works: The Science of Self-organized Criticality, Copernicus, New York, 1996.
[33] A. Vespignani, S. Zapperi, How self-organized criticality works: a unified mean-field picture, Phys. Rev. E 57 (1998) 6345.
[34] W.C. Abraham, M.F. Bear, Metaplasticity: the plasticity of synaptic plasticity, Trends Neurosci. 19 (1996) 126.
[35] S. Zapperi, K.B. Lauritsen, H.E. Stanley, Self-organized branching processes: mean field theory for avalanches, Phys. Rev. Lett. 75 (1995) 4073.
[36] A. Clauset, C.R. Shalizi, M.E.J. Newman, Power-law distributions in empirical data, ISAM Review 51 (2009) 661.
[37] D. Stauffer, A. Aharony, Introduction to Percolation Theory, Taylor & Francis, New York, 1994.
[38] S. Papanikolaou, F. Bohn, R.L. Sommer, G. Durin, S. Zapperi, J.P. Sethna, Universality beyond power laws and the average avalanche shape, Nat. Phys. 7 (2011) 316.
[39] D. Sornette, Critical Phenomena in Natural Sciences, Springer Verlag, Berlin, 2000.
[40] E. Lovecchio, P. Allegrini, E. Geneston, B.J. West, P. Grigolini, From self-organized to extended criticality, Front Physiol. 3 (2012) 98.
[41] J.J. Hopfield, A.V.M. Herz, Rapid local synchronization of action potentials: toward computation with coupled integrate-and-fire neurons, Proc. Natl. Acad. Sci. USA 92 (1995) 6655.
[42] A. Corral, C.J. Perez, A. Diaz-Guilera, A. Arenas, Phys. Rev. Lett. 74 (1995) 118.
[43] Z. Olami, H.J.S. Feder, K. Christensen, Self-organized criticality in a continuous, nonconservative cellular automaton modeling earthquakes, Phys. Rev. Lett. 68 (1992) 1244.
[44] S. Lise, H.J. Jensen, Transitions in non-conserving models of self-organized criticality, Phys. Rev. Lett. 76 (1996) 2326.

[45] H.M. Broker, P. Grassberger, Random neighbor theory of the Olami–Feder–Christensen earthquake model, Phys. Rev. E 56 (1997) 3944.
[46] M.L. Chabanol, V. Hakin, Analysis of a dissipative model of self-organized criticality with random neighbors, Rev. E 56 (1997) R2343.
[47] T.M. Fischer, D.E.J. Blazis, N.A. Priver, T.J. Carew, Metaplasticity at identified inhibitory synapses in Aplysia, Nature 389 (1997) 860.
[48] B.D. Philpot, K.K.A. Cho, M.F. Bear, Obligatory role of NR2A for metaplasticity in visual cortex, Neuron 53 (2007) 495.
[49] G. Turrigiano, S.B. Nelson, Homeostatic plasticity in the developing nervous system, Nature 5 (2004) 97.
[50] J.M. Beggs, N.M. Timme, Being critical of criticality in the brain, Front. Fractal Physiol. 3 (2012) 163.
[51] P.R. Huttenlocher, Synaptic density in human frontal cortex — development changes and effects of age, Brain Res. 163 (1979) 195.
[52] L.K. Low, H.J. Cheng, Axon pruning: an essential step underlying the developmental plasticity of neuronal connections, Phil. Trans. R. Soc. B 361 (2006) 1531.
[53] Y. He, Z. Chen, A. Evans, Structural insights into aberrant topological patterns of large-scale cortical networks in Alzheimer's disease, J. Neurosci. 28 (2008) 4756.
[54] A.G. Garrity, G.D. Pearlson, K. McKiernan, D. Lloyd, K.A. Kiehl, V.D. Calhoun, Aberrant "default mode" functional connectivity in schizophrenia, Am. J. Psychiatry 164 (2007) 450.
[55] H. Laufs, K. Hamandi, A. Salek-Haddadi, A.K. Kleinschmidt, J.S. Duncan, L. Lemieux, Temporal lobe interictal epileptic discharges affect cerebral activity in "default mode" brain regions, Hum. Brain Mapp. 28 (2007) 1023.
[56] I. Osorio, M.G. Frei, D. Sornette, J. Milton, Y.-C. Lai, Epileptic seizures: quakes of the brain? Phys. Rev. E 82 (2010) 021919.